

PAPERS | DECEMBER 01 2000

Experiments in statistical mechanics

Jeffrey J. Prentis



Am. J. Phys. 68, 1073–1083 (2000)

<https://doi.org/10.1119/1.1315604>



Articles You May Be Interested In

Why is the energy of motion proportional to the square of the velocity?

American Journal of Physics (August 2005)

Energy conservation in quantum mechanics

American Journal of Physics (May 2004)



Special Topic:
Teaching about the environment,
sustainability, and climate change

[Read Now](#)

Experiments in statistical mechanics

Jeffrey J. Prentis^{a)}

Department of Natural Sciences, University of Michigan–Dearborn, Dearborn, Michigan 48128

(Received 30 June 2000; accepted 21 July 2000)

We present experiments designed to illustrate the basic concepts of statistical mechanics using a gas of “motorized molecules.” Two molecular motion machines are constructed. The pressure fluctuation machine (mechanical interaction simulator) is a working model of two gases separated by a movable piston. The Boltzmann machine (canonical simulator) is a working model of a two-level quantum system in a temperature bath. Dynamical probabilities (fraction of time) are measured using mechanical devices, such as stop watches and motion sensors. Statistical probabilities (fraction of states) are calculated using physical statistics, such as microcanonical and canonical statistics. The experiments enable one to quantitatively test the fundamental principles of statistical mechanics, including the fundamental postulate, the ergodic hypothesis, and the statistics of Boltzmann. © 2000 American Association of Physics Teachers.

I. INTRODUCTION

If you measure the pressure p , volume V , mole number n , and temperature T of a gas in equilibrium and discover that $pV=nRT$, then this can be considered to be an indirect experimental test of the principles of statistical mechanics. If you could measure the amount of time $t(E)$ that a molecule of the gas spends in a quantum state of energy E and discover that $t(E)\sim\exp(-E/kT)$, then this would be a direct experimental proof of the basic principles of statistical mechanics, namely the ergodic hypothesis and Boltzmann statistics. The experiment that measures p , V , n , and T is a macroscopic experiment in thermodynamics. The theoretical journey that goes from $t(E)\sim\exp(-E/kT)$ to $pV=nRT$ is a long trek on a winding road. The experiment that measures $t(E)$ is a microscopic experiment in pure statistical mechanics—an experiment that focuses solely on statistical and mechanical concepts, without reference to thermal concepts. The primitive mechanical concepts are “time spent in a state” and “energy of a particle.” The primitive statistical concept is “Boltzmann statistics.”

In general, statistical mechanics is characterized by the mechanics of particles and the statistics of states. The basic mechanical object is the state of the system as a function of time: $s(t)$. All mechanical quantities, such as energy, depend on $s(t)$. The basic statistical object is the probability of the state: P_s . All statistical quantities, such as average and fluctuation, are determined from P_s . In contrast to statistical mechanics, the subject of thermodynamics is characterized by a set of thermal objects that describe the thermal properties of bulk matter: temperature T , pressure p , heat Q , work W , energy U , and entropy S .

An experiment in equilibrium statistical mechanics in its purest form is one in which $s(t)$ and P_s are directly measured. Such a pure statistical mechanics experiment, “uncontaminated” by thermal quantities, is rare. This is understandable given the impossibility of experimentally monitoring the dynamical behavior of each particle in a molar sample of matter. Thus in general, $s(t)$ and P_s are not observable. In fact, there exist several theoretical probability functions P_s (microcanonical, canonical, grand canonical) that yield, via a sum over states, the same thermodynamical observables (averages). In contrast to the scarcity of experiments in statisti-

cal mechanics, experiments in thermodynamics are commonplace. In the macroscopic world of thermal physics, there exist plenty of instruments that can readily measure the thermal properties of matter. Thermometers measure T , barometers measure p , and calorimeters measure Q . Unfortunately, there do not exist instruments to measure the mechanical and the statistical properties. It would be wonderful if there existed a “state-ometer” to measure $s(t)$ and a “prob-ometer” to measure P_s .

A few experiments in statistical mechanics exist. Perhaps the best known experiment is Brownian motion, first performed by Jean Perrin¹ and analyzed by Albert Einstein² as a proof of molecular reality. Demonstration apparatus is commercially available in which the Brownian motion of smoke particles is observed using a microscope.³ A laboratory experiment for undergraduate students has been developed to study the Brownian motion of polystyrene microspheres in water.⁴ A random walk experiment using a toy ball has been performed to illustrate the energy outflow in stars.⁵ Another experiment for the undergraduate laboratory is the sedimentation equilibrium of colloidal suspensions, whereby small plastic spheres suspended in a fluid form a miniature atmosphere.⁶ This type of experiment was suggested by Einstein and first performed by Perrin. The concentration of spheres is measured at different heights and found to obey a Boltzmann distribution. Demonstration equipment is also commercially available which illustrates the random motion of molecules by shaking a system of small balls.⁷ Similar equipment has been used to perform quantitative experiments which measure the velocity^{8,9} and height⁹ distribution of the “gas” of agitated balls. A transistor experiment that demonstrates the canonical distribution has recently been described.¹⁰

In this paper, we present two complete experiments in pure statistical mechanics—the pressure fluctuation machine and the Boltzmann machine. Each experiment involves a dynamical system whose mechanical $s(t)$ and statistical P_s properties are measured and analyzed.

II. THE SCIENCE OF STATISTICAL MECHANICS

In every branch of science, the scientific method generally consists of three basic ingredients: (1) Perform an experiment. (2) Formulate a theory. (3) Compare the experimental

observations with the theoretical predictions. For the purpose of organizing our experiments into a coherent whole, we define the science of statistical mechanics as follows. Let x denote the variable that labels the macrostate of a system. Let τ denote the total amount of time that the dynamics of the system is monitored and $\tau(x)$ the amount of time that the system spends in the macrostate x . Let Ω denote the total number of microstates accessible to the isolated system and $\Omega(x)$ denote the number of microstates accessible to the system when it is in the macrostate x . The scientific method of statistical mechanics consists of the following ingredients.

- (1) Experiment: Measure the time $\tau(x)$ and construct the dynamical probability $P_{\text{dyn}}(x) = \tau(x)/\tau$.
- (2) Theory: Count the states $\Omega(x)$ and construct the statistical probability $P_{\text{stat}}(x) = \Omega(x)/\Omega$.
- (3) Experiment versus theory: Is $P_{\text{dyn}}(x) = P_{\text{stat}}(x)$?

Note that the dynamical probability, $\tau(x)/\tau$, is a fraction of the *amount of time*, while the statistical probability, $\Omega(x)/\Omega$, is a fraction of the *number of states*. The conjectured equality of these two probabilities is a statement of the ergodic hypothesis.¹¹ Any experiment for which $\tau(x)$ can be measured and $\Omega(x)$ can be computed provides an experimental test of the ergodic hypothesis. In this paper, we measure $P_{\text{dyn}}(x)$, calculate $P_{\text{stat}}(x)$, and show $P_{\text{dyn}}(x) = P_{\text{stat}}(x)$.

In the standard undergraduate treatment of equilibrium statistical mechanics, the focus is on the statistics, rather than the mechanics. There is little discussion of the dynamical evolution of the state $s(t)$, the dynamical probability $\tau(x)/\tau$, the dynamical origin of the fundamental statistical postulate, or the ergodic hypothesis. And yet, these temporal features are the vital mechanical ideas that underlie all the statistical arguments and concepts. Although the thermodynamic observables of a macroscopic system in thermodynamic equilibrium are independent of time, the constituent particles of the system are forever moving through time. The fraction of time that the system spends in a state is the mechanical origin of the notion of probability in statistical mechanics. In our experiments, the dynamical objects, $s(t)$ and $P_{\text{dyn}}(x) = \tau(x)/\tau$, are directly measured using mechanical devices, such as rulers and clocks.

The key mechanical hardware in all our experiments is a motorized ball, known commercially as a Squiggle BallTM.¹² The ball has a mass of 120 g and a radius of 4 cm. It consists of a plastic spherical shell in which there is a battery-powered motor mounted along the axis. The motor rotates the shell at approximately 3 rev/s around the axis. When placed on a surface, the ball rolls, mostly without slip. A small rubber O-ring around the circumference of the shell provides the optimal grip. The maximum speed of the center of mass is approximately 1 m/s. When the ball collides with a wall, it rebounds in a random direction. When placed on the floor of a room with furniture or other obstacles, the ball will continue to move, never getting stuck anywhere. The ball moves with a distribution of speeds. Over time, the ball will eventually visit every square centimeter (cell) of the floor (phase space). In this sense, the ball dynamics is ergodic. Given the random and ergodic motion of this self-propelled ball, we call this ball a ‘‘motorized molecule.’’

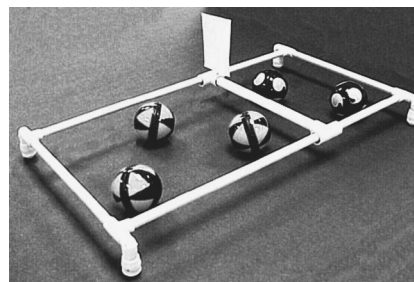


Fig. 1. Photograph of the pressure fluctuation machine (mechanical interaction simulator).

III. PRESSURE FLUCTUATION MACHINE

In this experiment, we study the mechanical interaction between two gases of motorized molecules. A picture of the apparatus is shown in Fig. 1. It consists of a rectangular frame constructed from PVC pipe (1/2 in. diameter). The frame is 68 cm long and 34 cm wide. In units of ball diameters, the frame is approximately eight balls long and four balls wide. The frame is elevated 6 cm above the ground using four PVC legs at each corner. The frame is placed on a level surface and the motorized molecules move on the surface within the rectangular frame. A movable wall, which acts as a piston, partitions the rectangular region into two regions. The wall consists of a 32-cm-long PVC pipe (3/4 in. diameter) fitted with *t*-joint connectors at each end. Each long pipe of the frame loosely fits through the hollow connectors allowing the joints to slide over the pipe and the wall to move freely. Many other mechanisms can be utilized for the sliding wall. We have also used pulleys riding on guide wires. Sliding-drawer tracks will also work. This apparatus, consisting of a rectangular frame, sliding wall, and motorized balls, constitutes a pressure-fluctuation machine that simulates the mechanical interaction between two gases separated by a movable piston.

The fundamental problem to be investigated both experimentally and theoretically with the mechanical interaction simulator is depicted in Fig. 2 and defined as follows:

Given: $N_L \equiv$ Number of balls on the left and $N_R \equiv$ Number of balls on the right.

Find: $P(x) \equiv$ Probability that the wall is at the position x .

The experiment consists of placing N_L motorized molecules in the left area and N_R motorized molecules in the right area, and monitoring the motion of the wall. The position of the wall as a function of time, $x(t)$, is measured using a motion detector. Such motion sensors are commercially

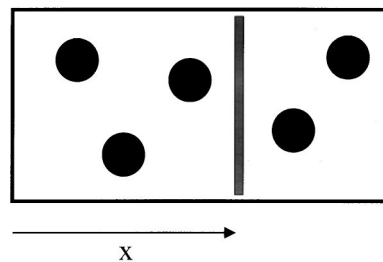


Fig. 2. Mechanical interaction between two gases of motorized molecules. The left gas has $N_L = 3$ molecules and the right gas has $N_R = 2$ molecules. The position x of the wall (piston) is the time-dependent variable that characterizes the fluctuating macrostate.

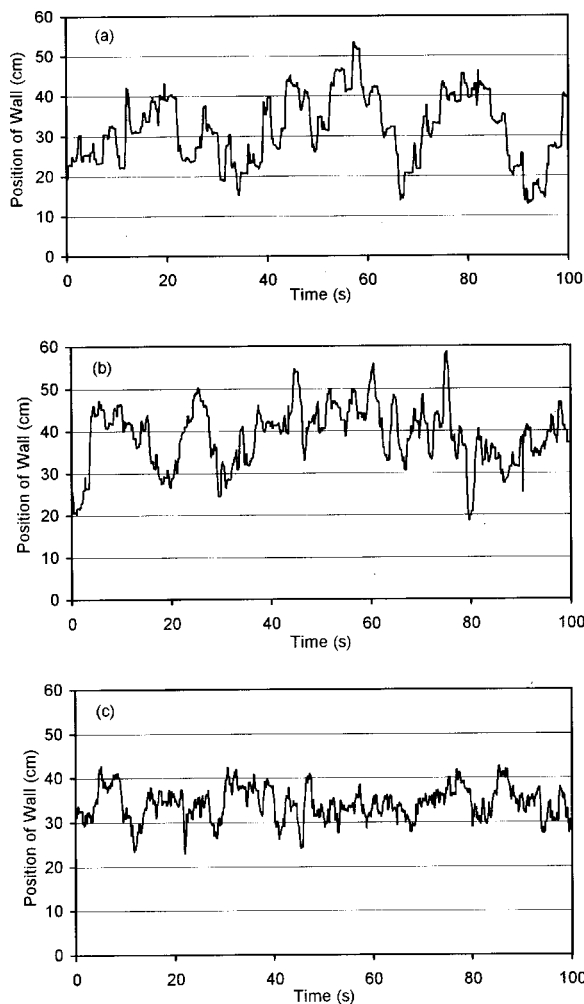


Fig. 3. Dynamics of the moving wall (position as a function of time) as measured with a motion detector for three different systems: (a) $N_L, N_R = 2,2$ (b) $N_L, N_R = 4,3$ (c) $N_L, N_R = 8,8$.

available and widely used in introductory physics laboratories.¹³ A small flag mounted on the wall provides the target for the sound pulses emanating from the motion detector. The motion detector collected data at the rate of 10 pulses per second. To minimize errors, the surface should be level, the frame should be stationary, the wall friction should be minimal and uniform, the batteries should be uniform in power, and the motion detector should be accurately zeroed.

We performed experiments to measure the dynamics of the wall for three different systems: $(N_L, N_R) = (2,2)$, $(4, 3)$, and $(8, 8)$. The position of the wall $x(t)$ as a function of time for these systems during the first 100 s is graphed in Fig. 3. A qualitative inspection of these world lines reveals that the average position of the wall is near the center of the apparatus for the $(2, 2)$ and $(8, 8)$ systems, and shifted to the right of center for the asymmetrical $(4, 3)$ system. Furthermore, the fluctuations around the average position decrease as more motorized molecules are added to the system.

The dynamical data for the position $x(t)$ of the wall can be represented as a probability distribution. In particular, we use a spreadsheet to convert the columns of the x vs t data into a histogram that gives the time $\tau(x)$ that the wall spends at a position between x and $x + \Delta x$. We have chosen the bin in-

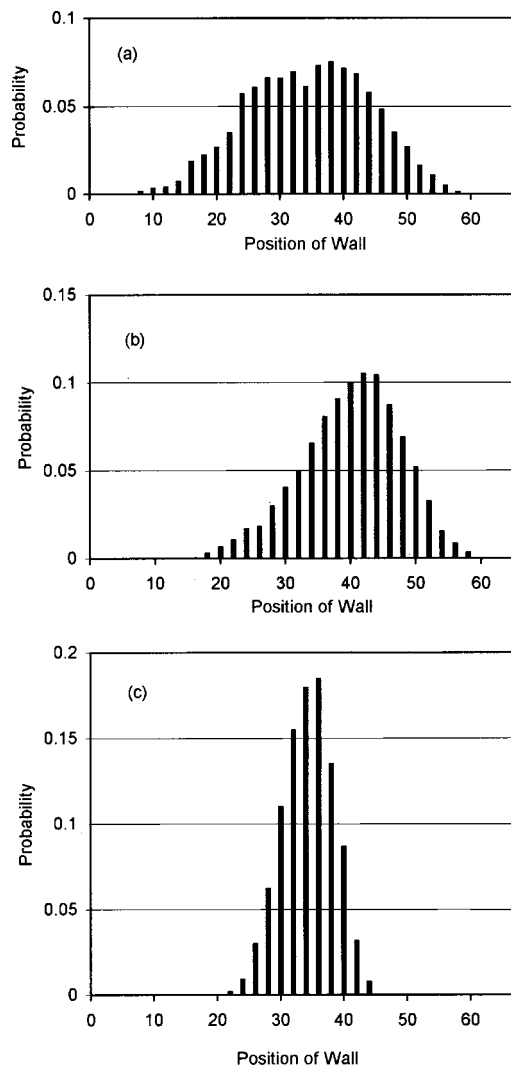


Fig. 4. Dynamical probability that the wall is at the position x for three different systems: (a) $N_L, N_R = 2,2$ (b) $N_L, N_R = 4,3$ (c) $N_L, N_R = 8,8$. The dynamical probability is the fraction of time that the wall spends at the position x . The probability graphs $P(x)$ represent the statistical behavior of the mechanical graphs $x(t)$ in Fig. 3.

terval Δx to be 2 cm, which is one-fourth the diameter of a ball. The dynamical probability to find the wall at a position between x and $x + \Delta x$ is

$$P_{\text{dyn}}(x) = \frac{\tau(x)}{\tau}, \quad (1)$$

where τ is the total observation time given by

$$\tau = \sum_x \tau(x). \quad (2)$$

For the $(2, 2)$ system and the $(4, 3)$ system, we monitor the dynamics for $\tau = 30$ min. For the $(8, 8)$ system, the observation time is $\tau = 45$ min. The dynamical probability functions $P_{\text{dyn}}(x)$ for these experiments are graphed in Fig. 4. The probability functions, $P_{\text{dyn}}(x)$, in Fig. 4 exhibit the statistical content of the dynamical functions, $x(t)$, in Fig. 3. In the experiments, one can vary the observation time τ . In the analysis, one can vary the bin interval Δx . We find that running the experiment for much shorter times, such as τ

Table I. Statistical parameters from the pressure fluctuation experiment.

N_L, N_R	$\langle x \rangle$ (cm)	σ (cm)
2, 2	33.5	9.64
4, 3	39.0	7.71
8, 8	33.3	4.12

=5 min, produces similar statistics—the same overall shape of $P_{\text{dyn}}(x)$ with similar average and fluctuation. Evidently, this time interval is sufficient to allow the system to cover a region of phase space that is a representative sample of the exact equilibrium distribution.

The average $\langle x \rangle$ and the fluctuation σ can readily be computed from the dynamical function $x(t)$ by summing over time, or equivalently from the statistical function $P_{\text{dyn}}(x)$ by summing over states:

$$\langle x \rangle \equiv \sum_x P_{\text{dyn}}(x)x, \quad (3)$$

$$\sigma^2 \equiv \sum_x P_{\text{dyn}}(x)(x - \langle x \rangle)^2. \quad (4)$$

The experimental values of these statistical descriptors are listed in Table I. As expected, the average position $\langle x \rangle$ of the wall is located at the center of the container for the (2, 2) system and the (8, 8) system, and displaced to the right of the center for the (4, 3) system. The fluctuations σ around the average are smaller for systems with a larger number of molecules. In particular, the relative fluctuation $\sigma/\langle x \rangle$ for the (2, 2), (4, 3), and (8, 8) systems are 29%, 20%, and 12%, respectively. The values of the average position of the wall that we have measured are such that when the wall is at these positions, the concentration of molecules (number per area) in the left area is equal to the concentration in the right area: $n_L = n_R$. The equality of n_L and n_R has a theoretical explanation, assuming that a system of motorized molecules obeys a two-dimensional ideal-gas equation of state of the form $p = nT$, where p is the pressure (force per unit length) on the wall. We also assume that the “temperature” T is constant ($T_L = T_R$) because the average speed of a motorized molecule is constant.¹⁴ Given these assumptions, the equality of concentrations, $n_L = n_R$, is equivalent to the equality of pressures, $p_L = p_R$. This is the statistical mechanical principle of mechanical equilibrium—the average (most probable) position of the wall occurs at a value for which the average force on the wall due to the left molecules is equal and opposite to the average force due to the right molecules. Thus our experimental results are consistent with the theoretical condition for the mechanical equilibrium of two interacting gases at constant temperature.

We now turn to the statistical mechanical theory that can explain the dynamical details (not just the average values) of the observed behavior of the fluctuating wall. The statistical probability to find the wall at a position x is

$$P_{\text{stat}}(x) = \frac{\Omega(x)}{\Omega}, \quad (5)$$

where $\Omega(x)$ is the number of microstates accessible to the system of balls when the wall is at x and Ω is the total number of microstates given by

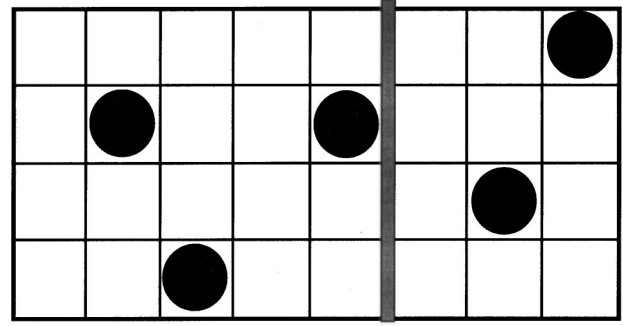


Fig. 5. Lattice (checkerboard) gas model of the mechanical interaction between two gases of motorized molecules.

$$\Omega = \sum_x \Omega(x). \quad (6)$$

Equation (5) is a symbolic statement of the fundamental postulate of statistical mechanics.¹⁵ In general, the fundamental postulate states that for an isolated system in equilibrium, each accessible microstate is equally probable. The number of microstates accessible to the composite system is a product of the number of microstates accessible to each subsystem:

$$\Omega(x) = \Omega_L(x, N_L) \cdot \Omega_R(x, N_R). \quad (7)$$

Thus to calculate the statistical probability $P_{\text{stat}}(x)$, one must count states.

The simplest model whose states can readily be enumerated is a lattice gas. Imagine partitioning the total area accessible to the moving balls into a lattice of sites, or a checkerboard of square cells as shown in Fig. 5. The length of the edge of each cell is equal to the diameter of the ball. The balls occupy the cells of the lattice, just as checkers occupy the squares of a checkerboard. Two balls cannot occupy the same cell. This digitization of the continuous area into a lattice of cells (sites) simplifies the counting of states. As an example, consider the situation shown in Fig. 5. The wall is at the lattice position $x=5$. In the left area, there are $N_L=3$ balls moving on 20 squares. In the right area, there are $N_R=2$ balls moving on 12 squares. The total number of microstates $\Omega(x)$ accessible to this system when the wall is at $x=5$ is

$$\Omega(5) = \Omega_L \cdot \Omega_R, \quad (8)$$

where

$$\Omega_L = 20 \cdot 19 \cdot 18,$$

$$\Omega_R = 12 \cdot 11.$$

Thus, for the macrostate $N_L=3, N_R=2, x=5$, the number of microstates is $\Omega(x)=902,880$. For positions of the wall that lie between the integer-valued lattice positions, one can still use this integer-valued counting algorithm. When the position of the wall changes by one bin interval distance $\Delta x=2$ cm, which is one-fourth the length of a cell, the area accessible to a ball changes by one lattice cell area. Thus the number of effective sites in the lattice takes on an integer value for each of the discrete values of the wall position x .

To justify this lattice model, we turn to classical statistical mechanics where the number of microstates is proportional to the area of phase space.¹⁶ Consider two balls, labeled 1

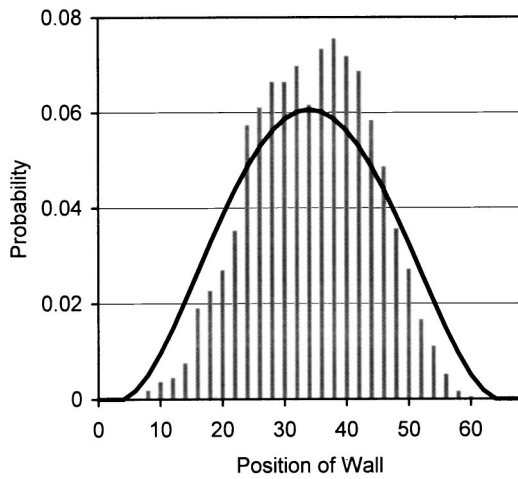


Fig. 6. Experimental dynamical probability (histogram) vs theoretical statistical probability (curve) for the system with $N_L, N_R=2,2$. The experimental histogram is measured using a motion sensor. The theoretical curve is calculated using the simple (zeroth-order) lattice gas model.

and 2, moving in a region of the plane. Let (x_1, y_1) and (x_2, y_2) denote the positions of the center of mass of each ball. Let A denote the area accessible to the center of mass of one ball moving in the region (without the other ball). Let the excluded area per ball be denoted by a and defined as the area that one ball excludes from the occupation by another ball. For now, assume that a is a constant. The number of microstates accessible to the two balls moving in this region is proportional to the positional area of phase space:

$$\int dx_1 dy_1 \int dx_2 dy_2 = A \cdot (A - a) = a^2 \left(\frac{A}{a}\right) \cdot \left(\frac{A}{a} - 1\right). \quad (9)$$

This continuum expression is equivalent to the lattice expression because the ratio A/a is the effective number of sites of the lattice. The proportionality constant a^2 is an irrelevant factor that cancels out in the ratio $\Omega(x)/\Omega$.

We have calculated the statistical probability function $P_{\text{stat}}(x)$ based on the simple method of counting states in the checkerboard model. The results for $(N_L, N_R) = (2, 2)$ are shown in Fig. 6. Similar results are obtained for the (4,3) system and the (8,8) system. For each system, the overall shape of the theoretical curve matches the profile of the experimental histogram. The mismatch occurs near the center (ends) of the probability curve where the theoretical values are smaller (larger) than the experimental values.

This lattice model is a simple (zeroth-order) approximation to the exact theory. The lattice statistics can be taught to students in introductory physics by analogy to the statistics of checkers on a checkerboard. One can formulate a more accurate theory by making modest corrections to this model. These corrections are due to the finite size of the ball. There are two important finite-size effects. First, the configurational phase-space area accessible to one ball is equal to the real-space area accessible to the center of mass of the ball. For example, if the moving ball is confined to a real-space area of dimensions 6×4 (in units of ball diameters), then the phase-space area is 5×3 . Second, the excluded area parameter a of a ball depends on the position of the ball. If a ball in the interior of the container excludes an area a , then a ball on the edge excludes an area $a/2$, and a ball in the corner ex-

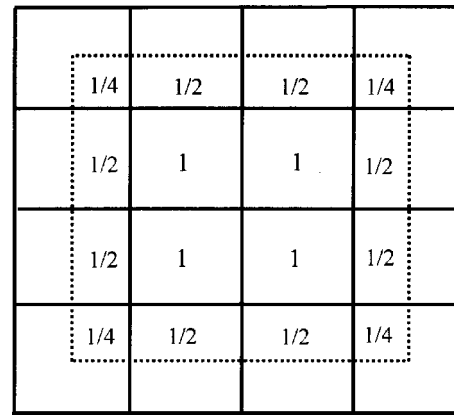


Fig. 7. Finite-size effects in the lattice-gas theory. The area accessible to the center of mass of a ball is the area enclosed by the dashed square. For the 4×4 lattice, this accessible (phase-space) area is equivalent to the geometric area of a 3×3 lattice. Cellular subsets of this area are labeled by the value of the exclusion parameter for interior cells (1), edge cells (1/2), and corner cells (1/4).

cludes an area $a/4$. These finite-size effects are illustrated in Fig. 7. Another finite-size effect occurs only when the wall is near the extreme ends of the apparatus and the balls are trapped so that they cannot move past one another. In effect, two trapped balls cannot exchange places, thereby making some microstates inaccessible.

To incorporate the finite-size effects into a theory, we modify the simple lattice gas theory described above. The simple lattice theory is characterized by two parameters—the size parameter, which is equal to the number of sites (square cells) accessible to the ball, and the exclusion parameter, which is equal to a constant value of 1 (one occupied square). Our modified theory preserves the checkerboard nature of the simple theory by merely modifying the values of the two checkerboard parameters. In the modified theory, the number of accessible sites is equal to the effective number of square cells accessible to the center of mass of the ball. To keep the calculations simple, we use an effective exclusion parameter equal to a constant value of $\frac{1}{2}$. This number represents a “mean-field” value of the possible values of the exclusion factor, 1, $\frac{1}{2}$, and $\frac{1}{4}$. The effective exclusion factor is an approximate average of the position-dependent exclusion factors over the possible positions of the ball and the wall. In this mean-field approximation, the value of $\frac{1}{2}$ for the lattice-model exclusion factor reflects the typical distribution of interior sites (1), edge sites (1/2), and corner sites (1/4) in the lattice.

It should be emphasized that this modified lattice gas theory is an approximate, coarse-grained version of the exact theory. To keep the theoretical analysis simple and pedagogical in this experimental paper, we have formulated a lattice theory that incorporates the important finite-size effects, and at the same time preserves the simple structural features and counting statistics of the checkerboard model. A more analytical kinetic theory of nonideal gases, such as van der Waals theory, would be difficult to apply to a system of motorized molecules because of their liquid-like concentrations. Furthermore, the dynamics of a motorized molecule is not the same as the dynamics of a real molecule. A rigorous classical theory, based on a continuum model, would involve the computation of phase-space integrals ($\int dq_1 dp_1 \cdots dq_N dp_N$) for a system of self-propelled hard

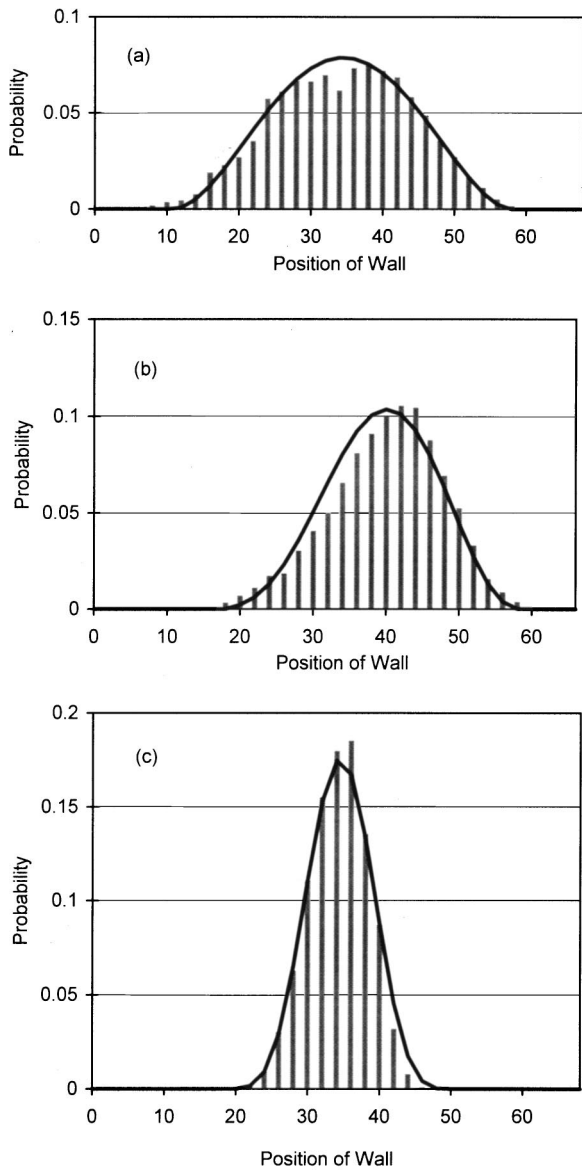


Fig. 8. Experimental dynamical probability (histogram) vs theoretical statistical probability (curve) for three different systems: (a) $N_L, N_R = 2, 2$ (b) $N_L, N_R = 4, 3$ (c) $N_L, N_R = 8, 8$. The dynamical probability is the fraction of the amount of time that the wall spends at each position. The statistical probability is the fraction of the number of microstates accessible to the system of balls for each position of the wall. The experimental histograms are measured using a motion detector. The theoretical curves are calculated using the modified lattice gas model.

spheres moving in a planar region. The integral (sum) over position states could be computed for a small number of spheres by directly enumerating (simulating) the possible configurations of the spheres. The integral (sum) over momentum states would be a challenge to compute without a detailed knowledge of the unnatural dynamics of the unnatural (motorized) molecules.

In Fig. 8, we display the results of our modified lattice gas theory. The agreement between the theoretical statistical probability and the experimental dynamical probability is good.¹⁷ Thus, this experiment provides an illustration of the ergodic hypothesis and the fundamental postulate of statistical mechanics.

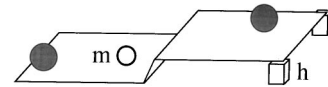


Fig. 9. The Boltzmann machine is a two-level dynamical system in which a particle (ping-pong ball of mass m) is free to make transitions between the lower ground level (energy 0) and the upper excited level (energy mgh) via collisions with its environment (motorized ball).

IV. BOLTZMANN MACHINE

The Boltzmann factor is one of the most potent and versatile factors in science. It governs the statistical mechanical behavior of all systems in nature that are exchanging energy with their environment. Although the Boltzmann factor is ubiquitous in theoretical physics, direct experimental tests of this factor are scarce.

We have designed a dynamical machine that simulates canonical statistics and provides a simple experimental test of the Boltzmann factor. A schematic version of this canonical simulator appears in Fig. 9. It consists of two horizontal surfaces separated by a vertical step of height h . A motorized ball is confined to each level. A ping-pong ball of mass m is free to move from one level to the other level via collisions with the motorized ball. The motorized ball acts as an agitator. In the language of statistical mechanics, the ping-pong ball is the system and the motorized ball is the environment. The lower level is the ground state (0) and the upper level is the excited state (1). The system “borrows” energy from the environment to make the transition from state 0 to state 1. The motor-ball environment acts as a reservoir in the sense that its average energy remains constant, independent of the energy exchanges with the ping-pong system.

A photograph of the actual Boltzmann machine appears in Fig. 10. Each level is constructed from a wooden board that is 33 cm long, 29 cm wide, and 2 cm high. Each board is made into a “boxing ring” so as to contain the balls. The boxing ring consists of a top and a bottom tier of rubber bands stretched between vertical nails mounted in each corner of the board. The bottom rubber-band wall confines the ping-pong ball, while the top rubber-band wall confines the motorized ball. The elasticity of the rubber-band walls helps to perpetuate the motion of the ping-pong ball. To help smooth out the motion around a corner, we have inserted a 6-cm-long rubber band into the corner so as to connect the two sides of the bottom wall, thereby rounding out the square corner. At the boundary between the levels, there is only the top rubber-band wall. This blocks the motorized ball and allows the ping-pong ball to pass. In effect, this boundary wall is a “semi-permeable membrane.” To achieve a smooth transition between the levels, we simply cover the surface with a piece of paper.

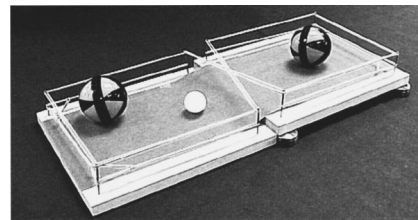


Fig. 10. Photograph of the Boltzmann machine (canonical simulator).

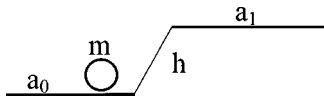


Fig. 11. Parameters that characterize the Boltzmann machine are the mass (m) of the ping-pong ball, the height (h) of the step, the surface area (a_0) of the lower level, and the surface area (a_1) of the upper level. The time that the ping-pong ball spends on each level, t_0 and t_1 , depends on m , h , a_0 , a_1 .

The fundamental Boltzmann problem to be studied both experimentally and theoretically using the Boltzmann machine is depicted in Fig. 11 and defined as follows:

Given: m ≡mass of the ping-pong ball, h ≡height of the step, a_0 ≡area of level 0, a_1 ≡area of level 1.

Find: t_0 ≡time that the ping-pong ball spends on level 0, t_1 ≡time that the ping-pong ball spends on level 1.

The experiment consists of monitoring the dynamics of the ping-pong ball. It is a simple procedure to watch the ball and record the amounts of time that it spends on the two levels, t_0 and t_1 , using a stopwatch. One person records t_0 and another person records t_1 . Alternatively, one person can perform the experiment by focusing on one level at a time. The person randomly rolls the ping-pong ball onto the level and then records the time it spends on the level before making the jump to the next level. This alternative procedure has the advantage of requiring the use of only one motorized ball on the level of interest. Using the same motorized ball on each level ensures that the distribution of speeds of the ping-pong ball on each level is the same. This ensures that the average kinetic energy of the ping-pong ball, or the “temperature,” is the same. This preserves the canonical picture of statistical mechanics in which the temperature of the system is constant. Since two motorized balls do not have exactly the same power and dynamical behavior, the temperature is not exactly the same on the two levels containing different motorized balls. In most cases, this slight difference in temperature has a negligible effect on the experimental results.

The results of our experiment using the Boltzmann machine are displayed in Table II. In this experiment, the areas of the two levels are equal. The same motorized ball is used on each level and the measurement of the time on each level is repeated 100 times. Two different masses (2.195 and 3.278 g) of ping-pong balls are used. Four different step heights (0, 0.525, 1.025, and 1.550 cm) are used. A variable-mass ping-pong ball can be made by inserting a thin, variable-length wire through a tiny hole in the ball so that the wire uniformly conforms to the inner spherical surface. Instead of ping-pong balls, we find that plastic golf balls also work well. It is important not to mix ping-pong balls and

Table II. Experimental data from the Boltzmann machine.

m (g)	h (cm)	mgh (μJ)	t_0/t_1
2.195	0	0	1.02
3.278	0	0	0.95
2.195	0.525	113	1.54
3.278	0.525	169	1.83
2.195	1.025	220	2.16
3.278	1.025	329	3.39
2.195	1.550	333	3.64
3.278	1.550	498	6.64

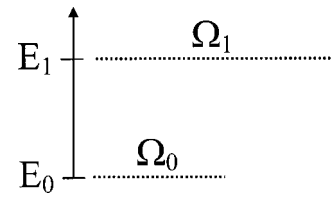


Fig. 12. The energy spectrum of the Boltzmann machine. Note the vivid similarities between the theoretical structure of the spectrum and the physical structure of the machine in Fig. 11. The spectral parts, $E_1 - E_0$ and Ω_1/Ω_0 , correspond exactly to the machine parts, mgh and a_1/a_0 , respectively.

golf balls in the same experiment because they have different dynamical (collisional) interactions with the motorized ball. In particular, because of the differences in size and elasticity, the average speed of a ping-pong ball is different than that of a golf ball having the same mass. The ratio of times t_0/t_1 that the ping-pong ball spends on the two levels is displayed in Table II. As we will show, this ratio can be calculated theoretically from the Boltzmann factor. The experimental value for the time ratio is obtained from the ratio of the total times that the ball spends on each level during the 100 jumps. For example, the time ratio $t_0/t_1 = 1.024$, corresponding to the smallest energy step $mgh = 0$, results from the ratio of $t_0 = 307.6$ s and $t_1 = 300.5$ s. The largest time ratio $t_0/t_1 = 6.64$, corresponding to the largest energy step $mgh = 498 \mu\text{J}$, results from the ratio of $t_0 = 2109.6$ s and $t_1 = 317.5$ s. In other words, for the energy step $mgh = 498 \mu\text{J}$, the average lifetime of the ping-pong ball in the ground state is 21.1 s, and the average lifetime in the excited state is 3.17 s.

Note that the value of the energy mgh in Table II is the characteristic energy gap separating the levels. It is the energy that the ping-pong ball must “borrow” from the motorized ball in order to make the transition from the lower level to the upper level. If the motion of the ping-pong ball obeys Boltzmann statistics, then, as we discuss later, the ratio of times t_0/t_1 should be an exponential function of the energy gap mgh . In particular, note that in Table II, there are two energy gaps ($mgh = 329$ and $333 \mu\text{J}$) that are approximately equal and that correspond to two different mass-height combinations, namely $(m, h) = (3.278 \text{ g}, 1.025 \text{ cm})$ and $(2.195 \text{ g}, 1.550 \text{ cm})$. For these energy gaps, the ratios of times ($t_0/t_1 = 3.39$ and 3.64) are also approximately equal.

We now turn to the statistical mechanical theory that can explain the observed dynamical behavior of the Boltzmann machine. In the language of quantum mechanics, the Boltzmann machine is a two-level system. The spectrum of states of this system is pictured in Fig. 12. A pedagogical value of the Boltzmann machine is that the two energy levels in energy space correspond to the two board levels in real space. Furthermore, the degeneracy of a level (number of quantum states, or area of classical phase space) is proportional to the surface area of the board. Thus there is a one-to-one mapping between the mechanical concepts (energy and degeneracy) and the architectural elements (step height and surface area). This correspondence is evident from looking at the machine schematic in Fig. 11 and the atomic spectrum in Fig. 12. The symbolic connection between the spectral parameters ($E_0, E_1, \Omega_0, \Omega_1$) and the machine parameters (m, h, a_0, a_1) is

$$E_1 - E_0 = mgh, \quad (10)$$

$$\frac{\Omega_1}{\Omega_0} = \frac{a_1}{a_0}. \quad (11)$$

This energy difference and degeneracy (multiplicity) ratio are the relevant mechanical inputs to the statistical mechanical theory.

In order to compare theory with experiment, we need to calculate the time that the ping-pong ball spends on the two levels. According to the ergodic hypothesis of statistical mechanics,¹¹ averages over time are equal to averages over (phase) space. An equivalent statement is that the time a system spends in a macrostate is proportional to the volume of phase space associated with the macrostate. In other words, the dynamical probability of a state is equal to the statistical probability of the state. Hence the ratio of times that the ping-pong ball spends on the two levels is equal to the ratio of statistical probabilities to find the ping-pong ball on the two levels:

$$\frac{t_0}{t_1} = \frac{P_0}{P_1}. \quad (12)$$

According to Boltzmann statistics, for any system in thermal equilibrium with a reservoir of temperature T , the probability for the system to have an energy E is $P(E) = \Omega(E) \times \exp(-E/kT)/Z$, where $\Omega(E)$ is the degeneracy, k is Boltzmann's constant, and Z is the partition function.¹⁸ Using this canonical probability, the ratio of times in Eq. (12) becomes a ratio of Boltzmann factors:

$$\frac{t_0}{t_1} = \frac{\Omega_0 \exp(-E_0/kT)}{\Omega_1 \exp(-E_1/kT)}. \quad (13)$$

This can be algebraically simplified to

$$\frac{t_0}{t_1} = \frac{\Omega_0}{\Omega_1} \exp[(E_1 - E_0)/kT]. \quad (14)$$

By substituting the energy difference and the multiplicity ratio from Eqs. (10) and (11) into Eq. (14), we arrive at¹⁹

$$\frac{t_0}{t_1} = \frac{a_0}{a_1} \exp(mgh/kT). \quad (15)$$

This is the basic theoretical equation that relates the dynamics (t_0, t_1) of the Boltzmann machine to the hardware parameters of its construction (m, h, a_0, a_1) . We will discuss the temperature parameter T later.

For the analysis of the experimental data, it is convenient to take the logarithm of the theoretical Eq. (15):

$$\ln\left(\frac{t_0}{t_1}\right) = \frac{1}{kT} mgh + \ln\left(\frac{a_0}{a_1}\right). \quad (16)$$

This expression provides an interesting relation between time (t) , energy (mgh/kT) , and entropy $(k \ln a)$, which we denote symbolically as

$$\text{Time} \Leftrightarrow \text{Energy} + \text{Entropy}.$$

In terms of the free energy $F \equiv E - TS$, Eq. (16) can be written in the condensed form

$$\ln\left(\frac{t_0}{t_1}\right) = \frac{\Delta F}{kT}, \quad (17)$$

where $\Delta E = mgh$ and $\Delta S = k \ln(a_1/a_0)$.

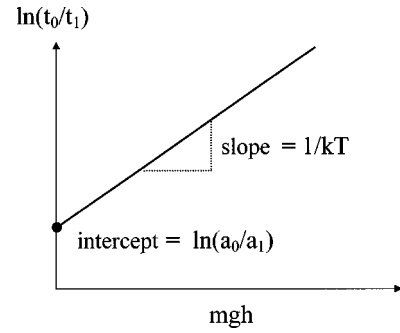


Fig. 13. According to the canonical theory (Boltzmann statistics) of the Boltzmann machine, a graph of $\ln(t_0/t_1)$ vs mgh is a straight line whose slope $(1/kT)$ provides information on the temperature and whose intercept $[\ln(a_0/a_1)]$ provides information on the entropy.

According to the canonical theory of Boltzmann, as represented by Eq. (16), a graph of $\ln(t_0/t_1)$ vs mgh should produce a straight line with a slope equal to $1/kT$ and an intercept equal to $\ln(a_0/a_1)$. The slope provides information on the energy and the intercept provides information on the entropy. A graph of the theoretical expression in Eq. (16) is shown in Fig. 13. A graph of the experimental data in Table II is shown in Fig. 14. The data points form a straight line. The best-fit line through the points is given by the equation $\ln(t_0/t_1) = 0.0038 mgh - 0.024$. Thus the dynamics of the Boltzmann machine obeys a Boltzmann distribution of temperature $kT = 260 \mu\text{J}$:

$$\frac{t_0}{t_1} = 0.98 \exp(mgh/260 \mu\text{J}). \quad (18)$$

The degeneracy ratio $a_0/a_1 = 0.98$ expresses the fact that the areas of the levels are equal within the uncertainties of the experiment. The area on which the motion occurs is subject to experimental uncertainty due to the small transitional area between the levels and the slightly changing shape of the elastic walls.

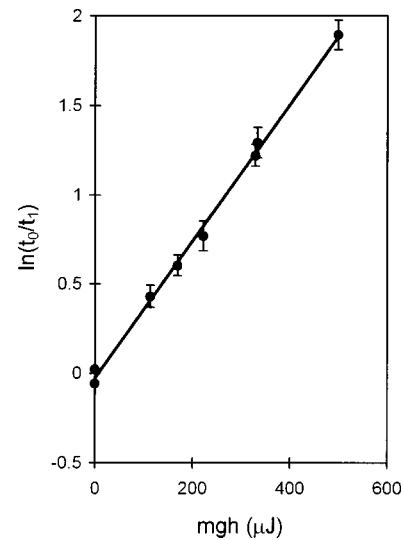


Fig. 14. The ratio of times spent on the two levels vs the energy gap between the levels. The experimental data points represent the Boltzmann machine data in Table II. The best-fit line through the data points is a Boltzmann distribution, $t_0/t_1 = (1/1.02) \exp(mgh/260 \mu\text{J})$.

What is the meaning of $kT=260 \mu\text{J}$? If we assume that the distribution of speeds of the ping-pong ball is a Boltzmann (Maxwellian) distribution, then according to the theorem of equipartition,²⁰ the average kinetic energy of the center of mass of the ping-pong ball moving in two (x,y) dimensions is

$$\langle \frac{1}{2}mv^2 \rangle = \langle \frac{1}{2}mv_x^2 \rangle + \langle \frac{1}{2}mv_y^2 \rangle = \frac{1}{2}kT + \frac{1}{2}kT = kT. \quad (19)$$

The fact that our data points for both the light and the heavy ping-pong ball lie on the same line provides experimental evidence that both ping-pong balls have the same “temperature.” Based on the experimental data (slope of line = $1/260 \mu\text{J}$), the average translational energy of both ping-pong balls is $\langle \frac{1}{2}mv^2 \rangle = 260 \mu\text{J}$. Hence, the root-mean-square speed of the light ($m=2.195 \text{ g}$) ping-pong ball is $v=49 \text{ cm/s}$. The root-mean-square speed of the heavy ($m=3.278 \text{ g}$) ping-pong ball is $v=40 \text{ cm/s}$. These values of the average speeds are consistent with the estimated values obtained from a qualitative observation of their motion. It is unlikely that the distribution of speeds of the ping-pong ball is exactly Maxwellian. The dynamics of a motorized molecule is not the same as that of a natural molecule. The collision between the motorized molecule and the ping-pong ball is not elastic. Nevertheless, one may assume an exponential, quasi-Maxwellian distribution of speeds parameterized by an effective temperature parameter $kT=260 \mu\text{J}$. There is other experimental evidence for a Maxwell-like distribution of speeds in a system of mechanically agitated balls.^{8,9}

We have performed another experiment to test the entropic contribution to the Boltzmann theory. The upper level of the Boltzmann machine is adjusted so that it has twice the surface area of the lower level.²¹ In theoretical language, this means that there is twice the classical phase-space area, or twice the number of quantum states accessible to the ping-pong ball when it is in the excited state. In symbols, the ratio of areas is $a_0/a_1 = \frac{1}{2}$. In running the experiment, it is important to place one motorized ball on the lower level and two motorized balls on the upper level so that the density of motorized balls is the same on both levels. This ensures that the distribution of speeds of the ping-pong ball is the same on both levels. In effect, the “temperature” of the entire system is constant. This is the vital canonical constraint. In our experiment, two boxing rings exist on the upper level, each confining one motorized ball. The “semi-permeable membrane” between the boxing rings blocks the motorized ball and allows the ping-pong ball to move freely on the entire surface. We measure the amount of time that the ping-pong ball spends on the upper level before it moves to the lower level. This measurement is repeated 100 times for the light and heavy ping-pong balls. The time spent on the lower level is taken from the first experiment. The experimental results are graphed in Fig. 15. The data points fall on a line described by the equation $\ln(t_0/t_1) = 0.0038 mgh - 0.71$. This best-fit line has the same slope as in the first experiment, but a different intercept. Thus the experimental data follow a Boltzmann distribution of temperature $kT=260 \mu\text{J}$ and degeneracy ratio $\Omega_0/\Omega_1 = 0.49$:

$$\frac{t_0}{t_1} = 0.49 \exp(mgh/260 \mu\text{J}). \quad (20)$$

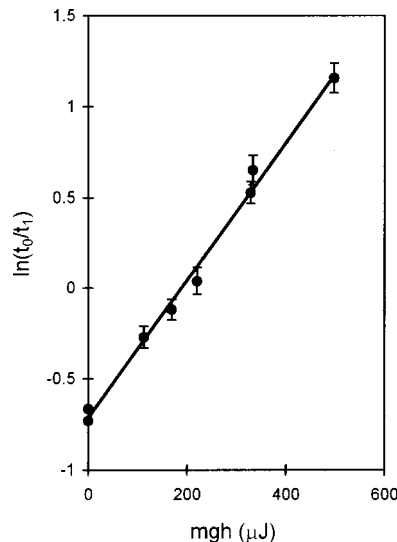


Fig. 15. The ratio of times spent on the two levels vs the energy gap between the levels. The experimental data points are the results of an experiment in which the surface area of the upper level of the Boltzmann machine is approximately twice the area of the lower level. The best-fit line through the data points is a Boltzmann distribution, $t_0/t_1 = (1/2.04)\exp(mgh/260 \mu\text{J})$.

This theoretical fit to the experimental data agrees with the actual parameters of the Boltzmann machine, namely that the ratio of the areas of the levels (a_0/a_1) is approximately equal to $\frac{1}{2}$. Note that the multiplicity factor (0.49) multiplying the Boltzmann factor in Eq. (20) is equal to one-half of the multiplicity factor (0.98) in Eq. (18).

We now describe a demonstration experiment that provides a vivid illustration of the concepts of dynamical equilibrium, transition rates, occupation numbers, and the canonical ensemble. The experiment involves running the Boltzmann machine with several ping-pong balls. Instead of focusing on the motion of one ball and the time it spends on each level, this experiment focuses on how the ensemble of balls populates the levels. For example, using nine of the light ping-pong balls ($m=2.195 \text{ g}$) in the Boltzmann machine with equal-area levels and the intermediate step height ($h=1.025 \text{ cm}$), the motion of the balls is such that, on average, there are six balls on the lower level and three balls on the upper level. This is shown schematically in Fig. 16. As a demonstration experiment, these average values represent approximate values obtained by direct observation and not elaborate measurements. The statistical fact that the lower level is populated with twice the number of balls as the upper

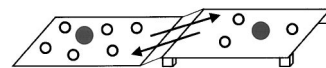


Fig. 16. Running the Boltzmann machine with several ping-pong balls illustrates the concepts of transition rates, detailed balance, occupation numbers, and the canonical ensemble. For a system of nine balls and an energy gap of $mgh=220 \mu\text{J}$, the average lifetime of a ball on the lower level (0) is approximately 6 s and the average lifetime on the upper level (1) is approximately 3 s. The equilibrium state is dynamically characterized by balls jumping between the levels at an average rate of approximately 1 ball/s, both in the forward direction ($0 \rightarrow 1$) and the reverse direction ($1 \rightarrow 0$). The equilibrium state is statistically characterized by a canonical population of the levels such that on average, six balls occupy the lower level and three balls occupy the upper level.

level is the ensemble version of the dynamical fact that each ball spends approximately twice the amount of time on the lower level than on the upper level. Indeed, from the Boltzmann machine data in Table II, the ratio of times for these values of m and h is $t_0/t_1=2.16$. In the language of atomic physics, the lifetime of a ball in the ground state is approximately twice the lifetime of the ball in the excited state. In the language of quantum statistics, the occupation number for the ground state is six and the occupation number for the excited state is three. The set of balls distributed in this way between the two levels represents a canonical ensemble of balls described by the Boltzmann factor $\exp(-mgh/260 \mu\text{J})$. One can further observe that the average rate (number of balls per unit time) at which balls jump from 0 to 1 (from lower level to upper level) is approximately equal to the rate at which balls jump from 1 to 0. The delicate balance between the forward and the reverse transitions (for every pair of states) is called the principle of detailed balance.²² It is a dynamical condition for thermal equilibrium (time-independent population of states). Thus, when the Boltzmann machine is run with several balls, the observer can literally see the dynamical process (detailed balance) whereby equilibrium is maintained. At the same time, the observer can see the statistical complement of this dynamical process, namely a canonical ensemble, or Boltzmann distribution of agitated balls.

V. CONCLUSION

The experiments presented in this paper are designed to illustrate the fundamental concepts and principles of statistical mechanics. The experiments focus solely on the mechanical and the statistical elements of statistical mechanics. There are no thermal objects, such as thermometers, calorimeters, or heating elements. There are no gambling objects, such as coins, dice, or cards. The notion of probability as the fraction of time that a system spends in a state is the hallmark of statistical mechanics that distinguishes physical statistics from mathematical statistics. This dynamical notion of probability is a common theme in the experiments presented in this paper. In each experiment, we use mechanical equipment (stopwatch, motion sensor) to measure $P_{\text{dyn}}(x) = \tau(x)/\tau$. We use physical statistics (fundamental postulate, Boltzmann statistics) to calculate $P_{\text{stat}} = \Omega(x)/\Omega$. In each experiment, we find $P_{\text{dyn}}(x) = P_{\text{stat}}(x)$. In this sense, these experiments provide simple and direct experimental proofs of the ergodic hypothesis, the fundamental postulate, and the statistics of Boltzmann. It should be noted that since these experiments utilize toy molecules and not real molecules, the experimental tests are toy tests and not real tests. Real tests of the foundations of statistical mechanics, in which the experimenter measures the motion of individual molecules in bulk matter, are virtually nonexistent. Insofar as real tests do not exist, it is gratifying that there exists a dynamical system, albeit a toy system, that illustrates the primitive foundations of statistical mechanics.

The experiments are low in technology and high in pedagogy. They can be used as demonstration equipment or as complete laboratory experiments in both introductory and advanced physics courses. Each experiment involves a holistic mix of experimental technique and theoretical analysis. By using “easy-to-see molecules” and simple devices to measure the “time spent in a state,” the experiments provide concrete imagery of abstract concepts. When the pressure

fluctuation machine is running, the observer directly sees the irregular motion of a piston in a gas and the molecular collisions that drive the motion. In essence, this device is a large-scale barometer, one in which the Brownian motion of the piston can be visualized, measured, and analyzed on the scale of human sensation, rather than on the anti-intuitive (nanometer) scale of atoms. Statistical mechanical concepts, such as probability, average, fluctuation, and equilibrium also take on a life-size meaning.

Similarly, the Boltzmann machine is a life-size dynamical simulator of Boltzmann statistics. It is a working model of a two-state atomic system in a temperature bath. The machine hardware mimics the spectral elements. The Boltzmann machine also represents a paradigm of nature—the ubiquitous process of “borrowing” energy. For most systems in nature, there exists a characteristic energy ΔE that the system must borrow from its environment in order to change its state. For example, in the atmosphere, the characteristic energy is the gravitational energy (mgh). In chemical reactions, the characteristic energy is the activation energy (E_a). In phase changes, the characteristic energy is the latent heat (L). In semiconductors, the characteristic energy is the energy gap (E_g). The Boltzmannian paradigm is as follows: The “price” that a system must pay to “borrow” an amount of energy ΔE from an environment of temperature T is proportional to $\exp(-\Delta E/kT)$. The relevant dimensionless parameter is $\Delta E/kT$, which can be interpreted as the ratio of the energy needed to the energy available. The Boltzmann machine is an archetypical device that illustrates the Boltzmannian paradigm. The operator of the Boltzmann machine can literally see the system (ping-pong ball) borrowing energy (mgh) from its environment (motorized ball), the dynamical mechanism (collisions) responsible for the energy exchange, and the resulting quantum jump (ground level to upper level). Watching the Boltzmann machine in action, one sees and hears a rather chaotic motion—balls banging into each other, randomly bouncing off walls, and moving with a variety of positions and velocities. It is gratifying to discover, both experimentally and theoretically, that there exists a statistical regularity in the dynamical data that brings an order to the chaos. This order in the dynamics is the statistics of Boltzmann.

Many other experiments in thermal and statistical physics can be performed using motorized molecules. The diffusive interaction between two gases can be studied. Liquids and solids can be simulated. Temperature effects can be studied by changing the speed of the molecular motor. Concepts of kinetic theory, such as mean-free path and diffusion, can be analyzed. We are currently finishing experiments for future publication on Brownian motion, polymer statistics, and the equation of state (pV diagram) of a gas of motorized molecules.

ACKNOWLEDGMENT

I would like to thank William Yuhasz for building the frame used in the pressure fluctuation experiment and for helping with the computer analysis.

^aElectronic mail: jprentis@umd.umich.edu

¹J. Perrin, *Atoms* (Ox Bow, Woodbridge, CT, 1990), pp. 109–133.

²A. Einstein, *Investigations on the Theory of the Brownian Movement* (Dover, New York, 1956), pp. 1–18.

³Cenco Brownian Movement Apparatus, No. 7127OU, Central Scientific Company, 3300 Cenco Parkway, Franklin Park, IL 60131.

- ⁴H. Kruglak, "Boltzmann's constant: A laboratory experiment," *Am. J. Phys.* **57**, 216–217 (1989).
- ⁵M. Zeilik, "Modeling Energy Outflow in Stars," *Phys. Teach.* **37**, 236–237 (1999).
- ⁶M. Horne, P. Farago, and J. Oliver, "An experiment to measure Boltzmann's constant," *Am. J. Phys.* **41**, 344–348 (1973).
- ⁷Molecular Motion Model, No. SF-8663, Pasco Scientific, 10101 Foothills Blvd., Roseville, CA 95747-7100. Molecular Motion Demonstrator, No. 31365, Central Scientific Company, 3300 Cenco Parkway, Franklin Park, IL 60131.
- ⁸H. Unruh and K. M. Unruh, "Experimental determination of the Maxwell velocity distribution," *Am. J. Phys.* **45**, 685–686 (1977).
- ⁹B. G. Eaton, R. G. Finstad, and P. D. Lane, "Kinetic theory simulator for laboratory use," *Am. J. Phys.* **47**, 132–135 (1979).
- ¹⁰M. D. Sturge and S. B. Toh, "An experiment to demonstrate the canonical distribution," *Am. J. Phys.* **67**, 1129–1131 (1999).
- ¹¹P. Ehrenfest and T. Ehrenfest, *The Conceptual Foundations of the Statistical Approach in Mechanics* (Dover, New York, 1990), pp. 21–26; Shang-keng Ma, *Statistical Mechanics* (World Scientific, Philadelphia, 1985), pp. 440–445; C. J. Thompson, *Mathematical Statistical Mechanics* (Macmillan, New York, 1972), pp. 214–217.
- ¹²Squiggle Ball™, distributed by Hart Enterprises Inc., 211 E. McLoughlin Blvd., Vancouver, WA 98663.
- ¹³Motion Sensor, No. CI-6742, Pasco Scientific, 10101 Foothills Blvd., Roseville, CA 95747-7100.
- ¹⁴For systems with larger asymmetry in the number of balls, such as $N_L, N_R = 4, 2$ or $6, 3$, it appears that $T_L \neq T_R$. In the $(4, 2)$ system, for example, the wall spends most of the time at a position that confines the two balls to a relatively small area, on the order of a couple of ball diameters in width. Based on observation, trapped balls tend to be less agitated. They have a smaller mean free path. Trapped balls move with a smaller average translational speed because they do not have enough area on which to gain momentum by rolling in the optimal orientation (along the O-ring). A molecule moving with a smaller speed exerts a smaller force on the wall. In effect, the "temperature" depends on the area of the gas. Thus, for the most probable state of asymmetrical systems ($N_L \neq N_R$), we conjecture that the gas in the left area and the gas in the right area are at different "temperatures." The equation of state of each gas has the form $p = nT$, where both n and T depend on the position x of the wall. For two gases at different temperatures, the mechanical equilibrium condition, $p_L = p_R$, assumes the form $n_L T_L = n_R T_R$. Thus, if $T_L > T_R$, then $n_L < n_R$. In physical (kinetic theory) terms, if the molecules in the right area are moving slower than the left molecules ($T_L > T_R$), then to achieve the same average force on the wall as the left molecules, the right molecules must collide with the wall at a higher rate than the left molecules ($n_L < n_R$). Further experiments are required to test this hypothesis.
- ¹⁵F. Reif, *Fundamentals of Statistical and Thermal Physics* (McGraw-Hill, New York, 1965), p. 54.
- ¹⁶K. Stowe, *Introduction to Statistical Mechanics and Thermodynamics* (Wiley, New York, 1984), pp. 13–17.
- ¹⁷For the asymmetric system ($N_L, N_R = 4, 3$), the theoretical curve is slightly displaced (about 2 cm) to the left of the experimental histogram. Although this may be due to the approximations in our lattice theory or a systematic error in the experiment, it is what one would expect in view of the comments in Ref. 14. A system of motorized molecules is a nonideal gas. The energy E of this gas depends on the area A of confinement. A rigorous theory of asymmetric systems ($N_L \neq N_R$) would need to analyze the dynamics of motorized molecules in order to obtain information on the energy function $E(A)$. Knowledge of $E(A)$ is needed to calculate $P(x)$. More specifically, the wall probability function has the general form $P(x) = \Omega_L(E_L, A_L, N_L) \Omega_R(E_R, A_R, N_R) / \Omega$, where the areas and the energies depend on x . For symmetric systems ($N_L = N_R$), this energy effect (or momentum phase-space effect) is less important because the wall spends most of the time at values of x for which the energy is approximately constant, independent of these (most probable) values of x .
- ¹⁸See Ref. 15, p. 205.
- ¹⁹In the canonical probability function, $P(E) = \Omega(E) \exp(-E/kT) / Z$, the energy of the ping-pong ball is $E = \frac{1}{2}mv^2 + \frac{1}{2}I\omega^2 + mgh$. In the level-probability ratio P_0/P_1 , the kinetic energy contribution cancels because the set of momentum states in phase space for the ball on the lower level is equal to the set on the upper level. The relevant contribution to the physical statistics comes from the set of position states in phase space for each level which is characterized by an energy difference mgh and an entropy difference $k \ln(a_1/a_0)$.
- ²⁰See Ref. 15, pp. 248–250.
- ²¹We have constructed a "variable-entropy" Boltzmann machine whose upper level can be adjusted to form regions of different shapes and sizes. The upper level consists of a large board, approximately twice the length of the lower board. A series of nails mounted along the perimeter of the upper board allows the operator to stretch elastic bands between different nails, thereby changing the geometry of the upper level.
- ²²See Ref. 15, pp. 548–553.